A General Methodology for the Synthesis of Transition Metal Pnictide Nanoparticles from Pnictate Precursors and Its Application to Iron−Phosphorus Phases

Kimber L. Stamm,[†] Jayne C. Garno,[†] Gang-yu Liu,[‡] and Stephanie L. Brock*,[†]

Department of Chemistry, Wayne State University, 5101 Cass Avenue, Detroit, Michigan 48202, and Department of Chemistry, University of California, Davis, One Shields Avenue, Davis, California 95616

Received August 16, 2002; E-mail: sbrock@chem.wayne.edu

Three-dimensional limiting of extended solids to produce nano-particles has a profound influence on the magnetic, electronic, and optical properties of a material.[1,2] The study of such size-dependent phenomena is predicated on access to well-defined materials and impacts both advancements in existing technologies (e.g. the effect of decreasing bit size on device performance) as well as new, unanticipated technologies. Although general routes to nanoparticles of main group pnictides (pnicogen = group 15 element) such as InP and GaAs have been developed,[3,4] nanoparticles of transition metal analogues remain largely unexplored. This is surprising because bulk transition metal pnictides exhibit properties of significant interest including ferromagnetism, magnetoelastic and magnetooptical properties, semiconductivity, and superconductivity.[5] Understanding size-dependent phenomena in nanocrystalline transition metal pnictides may contribute to the advancement of technologies, such as magnetoresistive sensing, magnetic refrigeration, and data storage and transmission. However, the lack of synthetic methodologies has severely limited the opportunities for systematic exploration of the size-dependent physical properties in these materials.[6]

The reduction of transition metal pnictates (other than nitrate) to pnictides is a proven route to bulk, microcrystalline pnictide phases of Fe, Co, W, and Mo, among others.[7] We are interested in exploiting this method for the facile production of transition metal pnictide nanoparticles by using preformed transition metal pnictate nanoparticles as precursors. This route should be general for a number of transition metals and pnicogens and has the benefit of avoiding the use of highly toxic and pyrophoric agents such as $P(SiMe_3)_3$, commonly employed in main group nanoparticle synthesis.[3,4] Additionally, the method is expected to permit control of stoichiometry, an important criterion as the phase diagrams of transition metal pnictides are considerably richer than their main group congeners. As proof of concept, we report herein the application of pnictate reduction to the synthesis of transition metal pnictide nanoparticles, specifically, the magnetic iron phosphides FeP and Fe_2P.[8]

The precursor iron phosphate nanoparticles were produced by a route analogous to that reported for the synthesis of $LaPO_4$ nanoparticles,[9] and the morphology and size were determined using atomic force microscopy (AFM).[10] Figure 1A reveals the typical morphology of these nanoparticles to be nearly spherical. Particle diameter was measured from the height in the cursor profiles as illustrated in Figure 1B[11] and was found to range in size from 1.4 to 4.6 nm, with an average value of 2.8 ± 0.6 nm for this sample.

Reduction of precipitated particles in H_2/Ar atmosphere produced crystalline patterns of phase-pure FeP (700 °C) and Fe_2P (1100 °C) (Figure 2).[12] However, the sharp diffraction patterns are
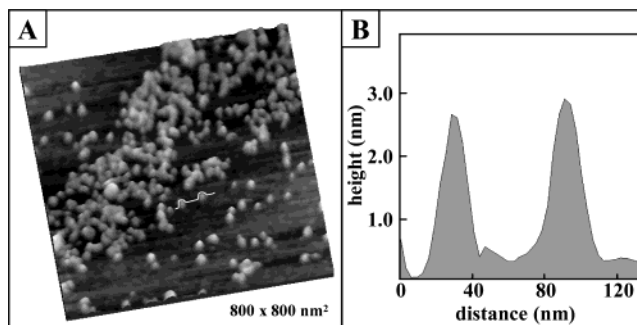
† Wayne State University.
‡ University of California, Davis.

Figure 1. AFM study of iron phosphate nanoparticles. (A) An 800×800 nm^2 topographic image. (B) Cursor profile of two nanoparticles from (A), measuring 2.7 and 2.9 nm, respectively.
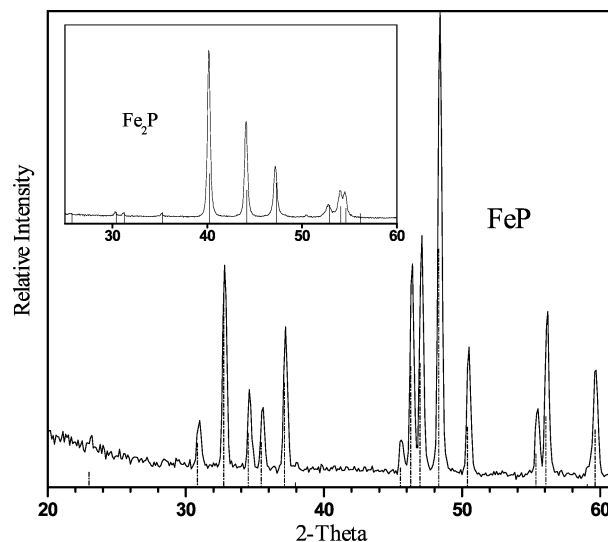

Figure 2. X-ray diffraction patterns of precipitated iron phosphate nanoparticles annealed under H_2/Ar at 700 and 1100 °C (inset), and corresponding line diagrams for FeP (78−1443) and Fe_2P (85−1725).[13]

indicative of the formation of large crystallite sizes (>500 nm), indicating that sintering has occurred. The presence of crystalline phosphates such as $Fe_2(P_4O_{12})$ (powder diffraction file (PDF): 76−0223) at temperatures of ca. 400 °C, in turn, suggests that the sintering occurs well before reduction to the pnictide.[13] Between 800 and 1000 °C, both FeP and Fe_2P are observed, suggesting transformation from FeP to Fe_2P with loss of phosphorus as a volatile byproduct (likely as phosphine).[12]

To prevent sintering, we have begun to explore techniques for preventing aggregation during reduction by increasing the interparticle separation and/or restricting the particle mobility. These can be achieved by decreasing particle concentration during
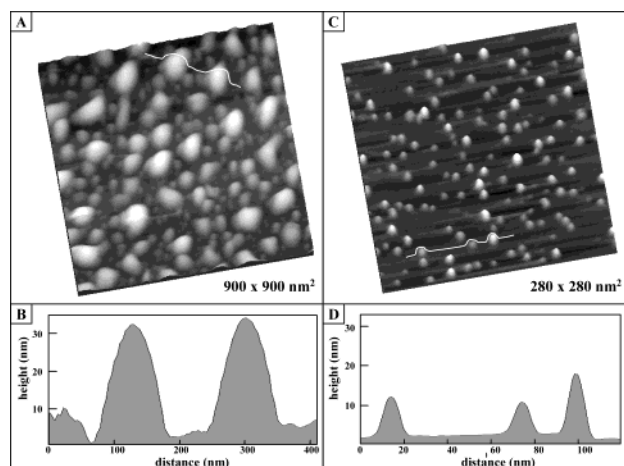
Figure 3. AFM topographic study of the particles after annealing. Surface-confined precursors were calcined at 700 °C for 1 h, in 7% hydrogen in nitrogen. (A) Precursor concentration: 2.3 mg/mL. (B) Cursor profile from (A). (C) Precursor concentration: 0.19 mg/mL. (D) Cursor profile from (B).

reduction and confining the particles on surfaces, respectively.[14] Accordingly, particles were reductively annealed directly on the mica substrate.

The results of directly annealing surface-confined phosphate nanoparticle precursors at 700 °C are illustrated in Figure 3.[15] At high initial coverage, the resulting iron phosphide particles are 3D aggregates ranging from 0.8 to 37 nm (average 13.4 ± 8.7 nm) as shown in Figure 3A. Quantitative measurements of two relatively large particles are shown in Figure 3B. The scale of these 3D aggregates represents a significant growth in particle size relative to the phosphate precursor employed for this experiment (2.18 ± 1.3 nm). However, at low coverage, phosphide nanoparticles exhibit a near-spherical morphology with an average size of 1.41 ± 0.5 nm, as shown in Figure 3C and D. Assuming spherical geometry, we found that annealing results in 35% reduction in particle diameter (~75% reduction in volume), consistent with oxygen loss during the transformation of phosphate to phosphide (predicted volume reduction from $FePO_4$: 72% for FeP, 79% for Fe_2P). On the basis of data obtained for sintered samples (Figure 2), the expected phase at 700 °C is FeP.[16]

The reduction of phosphorus is further confirmed in the XPS spectra (Supporting Information). The P 2p XPS spectrum reveals two peaks at 132.7 and 128.4 eV, respectively, with an intensity ratio of 70:30. The lower energy peak is consistent with the binding energy for FeP (129.5 eV),[17] demonstrating that some reduction has occurred. The presence of oxidized phosphorus (132.7 eV) is not unexpected as the samples are exposed to air during introduction to the XPS chamber. These data, including the observation of oxidation, are consistent with those observed for other phosphide nanoparticles (e.g., InP).[3]

In conclusion, the preparation of iron phosphide nanoparticles presented here represents the first report of the use of preformed nanoparticle precursors for the synthesis of nanoparticulate pnictides. However, this general methodology is expected to be applicable to a wide range of transition metals and pnicogens. To date, we have successfully extended this approach to Ni–As nanoparticulate phases and are also investigating other strategies for limiting aggregation, including solution reduction routes, to further expand the versatility of the method.

Supporting Information Available: XPS spectra of Fe–P samples reduced on mica (PDF). This material is available free of charge via the Internet at http://pubs.acs.org.

References

(1) Leslie-Pelecky, D. L.; Rieke, R. D. *Chem. Mater.* **1996**, *8*, 1770–1783.
(2) Alivisatos, A. P. *J. Phys. Chem.* **1996**, *100*, 13226–13239.
(3) Guzelian, A. A.; Katari, J. E. B.; Kadavanich, A. V.; Banin, U.; Hamad, K.; Juban, E.; Alivisatos, A. P.; Wolters, R. H.; Arnold, C. C.; Heath, J. R. *J. Phys. Chem.* **1996**, *100*, 7212–7219.
(4) (a) Mićić, O. I.; Curtis, C. J.; Jones, K. M.; Sprague, J. R.; Nozik, A. J. *J. Phys. Chem.* **1994**, *98*, 4966–4969. (b) Coffer, J. L.; Johnson, M. A.; Zhang, L.; Wells, R. L.; Janik, J. F. *Chem. Mater.* **1997**, *9*, 2671–2673. (c) Kher, S. S.; Wells, R. L. *Nanostruct. Mater.* **1996**, *7*, 591–603. (d) Peng, X.; Wickham, J.; Alivisatos, A. P. *J. Am. Chem. Soc.* **1998**, *120*, 5343–5344.
(5) Hulliger, F. *Struct. Bonding* **1968**, *4*, 83–229.
(6) (a) Previous reports of the synthesis of transition metal pnictide nanoparticles have been limited to organometallic pyrolysis routes[6b] and solvothermal syntheses.[6c,d] (b) Lukehart, C. M.; Milne, S. B.; Stock, S. R. *Chem. Mater.* **1998**, *10*, 903–908. (c) Xie, Y.; Lu, J.; Yan, P.; Jiang, X.; Qian, Y. *J. Solid State Chem.* **2000**, *155*, 42–45. (d) Xie, Y.; Lu, J.; Yan, P.; Jiang, X.; Qian, Y. *Chem. Lett.* **2000**, 114–115.
(7) Gopalakrishnan, J.; Pandey, S.; Rangan, K. K. *Chem. Mater.* **1997**, *9*, 2113-2116.
(8) Fe_2P is ferromagnetic, $T_c = 266$ K, and FeP is antiferromagnetic, $T_N = 125$ K; other phases in the Fe–P phase diagram: FeP_2 (semicond.) and Fe_3P (ferromagnetic, $T_c = 716$ K).[5]
(9) (a) $FeCl_3$ was treated with crystalline H_3PO_4 and tri-*n*-octylamine in tris-2-ethylhexylphosphonate (TEHP) at 160 °C overnight, followed by precipitation with methanol. The resultant nanoparticles have an Fe:P ratio of $0.92 \pm 5\%$ (ICP-MS) and are soluble in pyridine, toluene, or hexane. (b) Riwotzki, K.; Meyssamy, H.; Kornowski, A.; Haase, M. *J. Phys. Chem. B* **2000**, *104*, 2824–2828.
(10) (a) Samples for AFM were prepared by depositing a 10 μL drop of phosphate nanoparticle solution onto freshly cleaved mica (0001) surfaces, followed by air-drying. The AFM scanner is home-constructed and employs the optical beam-deflection configuration.[10b,c] The electronic controllers and software are from RHK Technology, Inc. Commercially available Si_3N_4 cantilevers with force constants of 0.1 N/m (microsharpened cantilever, Thermo Microscopes) were used for imaging. The AFM scanner was calibrated using Au(111) periodicity and step height. Contact-resonance imaging (CRI) was used to minimize adhesion between the tip and surface, thus circumventing stick-slip motion during scanning.[10d] (b) Kolbe, W. F.; Ogletree, D. F.; Salmeron, M. B. *Ultramicroscopy* **1992**, *42*, 1113–1117. (c) Liu, G.-Y.; Fenter, P.; Chidsey, C. E. D.; Ogletree, D. F.; Eisenberger, P.; Salmeron, M. *J. Chem. Phys.* **1994**, *101*, 4301–4306. (d) Wadu-Mesthrige, K.; Amro, N.; Garno, J. C.; Cruchon-Dupeyrat, S.; Liu, G.-Y. *Appl. Surf. Sci.* **2001**, *175*–*176*, 391–398.
(11) Lateral AFM sizes are a convolution of tip geometry. Without aggressive deconvolution, it is more reliable to use measurements of nanoparticle heights. Over 150 cursor profiles were analyzed for average particle size determinations.
(12) **Safety Note:** Because of the use of hydrogen mixtures (7–15% in Ar or N_2), as well as the possibility of producing toxic byproducts (e.g., PH_3), all reduction reactions were either conducted in, or vented to, a fume hood.
(13) Powder diffraction file (PDF) data were obtained from the ICDD-PDF database, release 2000.
(14) Chen, Z. X.; Smith, G. C.; Putman, C. A. J.; ter Voert, E. J. M. *Catal. Lett.* **1998**, *50*, 49–57.
(15) AFM imaging of plain mica substrates indicates that the surface remains atomically flat under the annealing conditions employed here.
(16) Although both iron and phosphorus are detected, the stoichiometry of the reduced nanoparticle phase on mica (FeP, Fe_2P) has not been determined due to sensitivity issues with conventional methods (e.g., XPS) on these highly dilute samples. Planned magnetic studies[8] will probe whether the reduction temperature dependence of the phase transformation is identical to that observed in the bulk, or if there are differences due to size effects, and this will be presented in a full paper.
(17) Binding energy data are available online at http://srdata.nist.gov/xps/.

JA028180V